DRAFT COPY

Polarization loss compensation in a laser transceiver system

Jeffrey M. Hoffman
Optical Research Associates, 5210 East Williams Circle, Suite 610, Tucson, Arizona 85711
E-mail: jeffh@opticalres.com

Norman A. Page
NASA Jet Propulsion Laboratory, 4800 Oak Grove Drive, Pasadena, California 91109
E-mail: norman.a.page@jpl.nasa.gov

ABSTRACT

JPL is developing a polarization-based sky tracking laser transceiver system in which some mirror coatings produce significant polarization losses that vary with tracking angle. We describe a useful method for dynamically compensating these effects.

Keywords: Optical communications, Optical systems design, Polarization

1. Introduction

The Jet Propulsion Laboratory (JPL) is developing a laser transceiver system, the Optical Communications Telescope Laboratory (OCTL), which will be used to investigate communications methods to support future NASA missions. The system consists of a Nd:YAG laser operating at a wavelength of 532 nm or 1064 nm, a series of beam-processing optics, and a 1-m diameter telescope mounted in an elevation/azimuth mount with fast sky tracking capability. The system sends four circularly polarized beams up to an Earth-orbiting satellite. Cube corner retro-reflectors on the satellite return the beams to the same telescope, and a polarization beam splitter diverts the returned light to a detection channel. To maximize round-trip transmission efficiency and to minimize variations in transmission with tracking angle, the optical components should maintain the polarization characteristics of the uplink and downlink beams. Modification of the polarization state by an optical component will result in signal loss at the polarization beam splitter.

As part of a detailed transmission and polarization analysis of the system performed by Optical Research Associates (ORA), we found that most of the optical components did not significantly affect the polarization states of the uplink and downlink beams. However, we found that a series of 45° mirrors used as part of the elevation/azimuth mount did produce significant polarization losses. These mirrors are coated with high-reflectance protected silver coatings, and JPL does not have the option to replace the mirrors. Without compensation, the polarization retardance produced by these mirrors results in large polarization losses that vary as a function of elevation and azimuth angle, as well as source wavelength.

Here, we describe two methods that we developed for compensating the phase retardance produced by the fold mirrors. The first is a straightforward application of three linear retarders with custom retardance values, and the second is an improved approach that uses a half wave plate (HWP) and a quarter wave plate (QWP) mounted in separate rotation stages. Both approaches provide dynamic compensation for polarization error as the telescope tracks across the sky; however, the second method allows the use of off-the-shelf components and can be adjusted to account for differences in retardance values produced by the mirrors from the expected values. We will describe each compensation method and describe methods for calculating the necessary rotation angles for the wave plates.

2. OCTL optical system description

The OCTL optical system, designed by Norman Page at JPL, uses a high-energy Nd:YAG laser source operating at either 532 nm or 1064 nm. The beam is divided into four separate beams that are used to test methods for mitigating the effects of atmospheric scintillation[2]. The beam-processing optical components and laser source are designed to fit onto a 5 × 8 foot optical table, as shown in Figure 1.

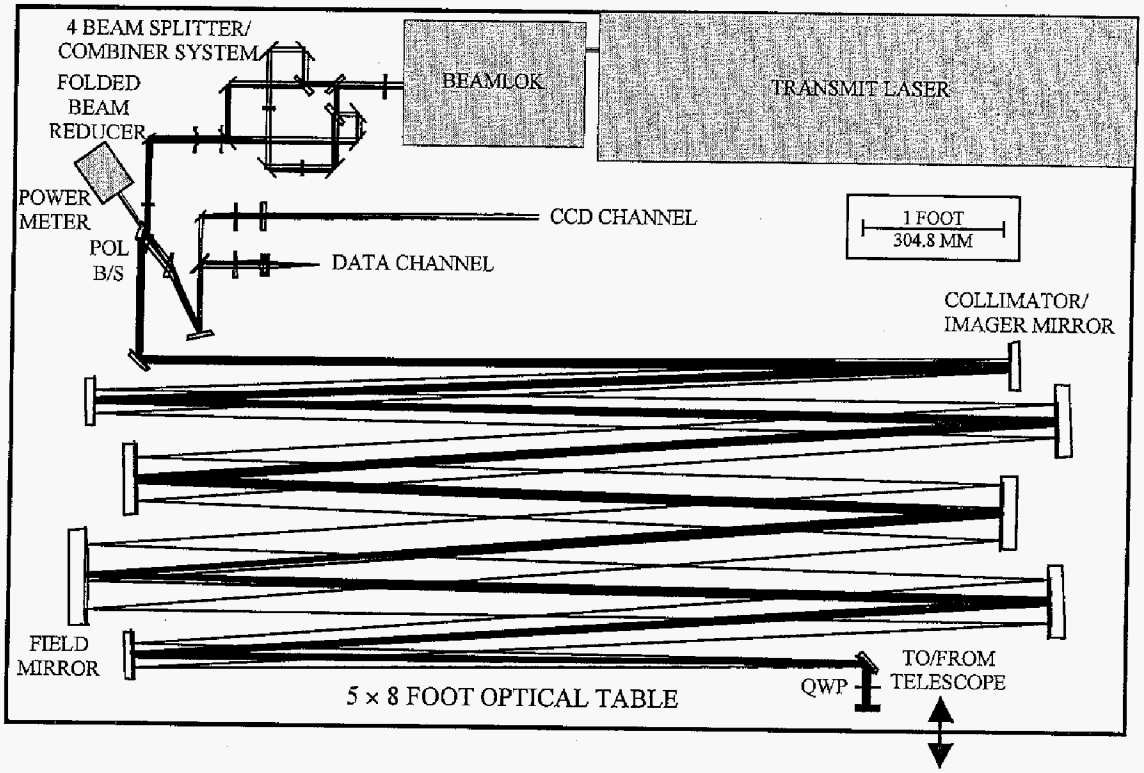

Figure 1. The layout for the beam processing optics is shown from the laser source to the input of the elevation/azimuth mount.

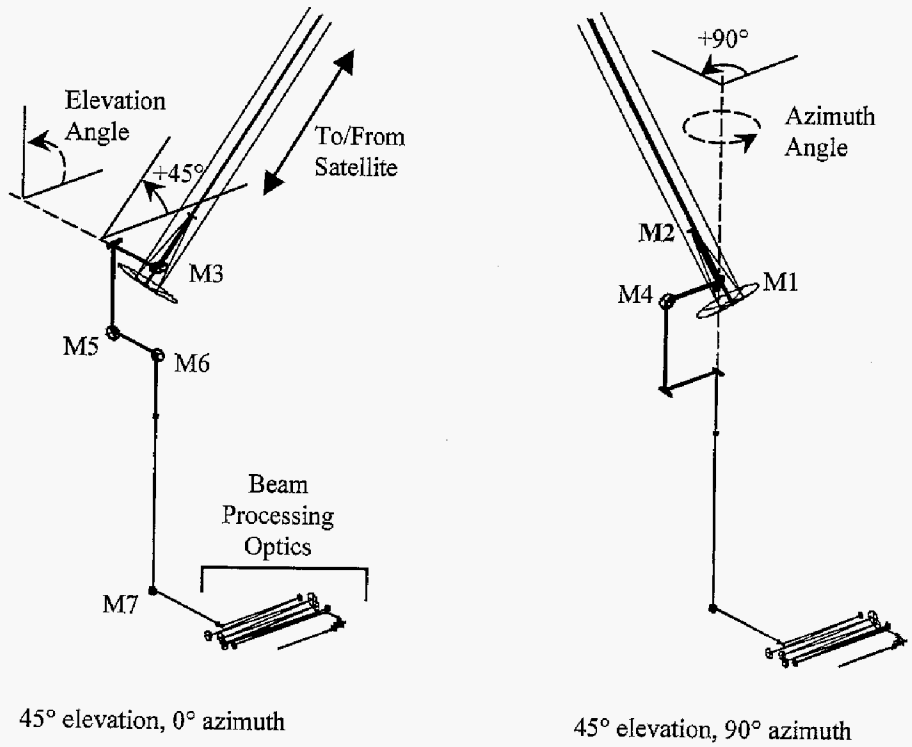

Figure 2. The telescope and Coudé optics are shown versus telescope pointing. Rotation with elevation angle rotates Mirror M3 relative to the other 45° mirrors, and rotation with azimuth angle rotates Mirrors M3 to M6 relative to Mirror M7.

The output beam passes from the optical table through a series of five 45° fold mirrors to a 1-m diameter Cassegrain telescope, as shown in Figure 2. For this discussion, we have labeled the seven mirrors from the telescope primary to the Coudé optics M1 to M7, where M1 and M2 are the telescope primary and secondary mirrors, the group of mirrors from M1 to M3 rotate to provide elevation angle control, and the group of mirrors from M1 to M6 rotate for azimuth angle control. Two examples of telescope pointing angle are shown in Figure 2 to show how the mirrors are rotated with respect to each other.

The uplink beam is p-polarized following the polarization beam splitter and is converted to circularly polarized by the quarter wave plate before exiting the telescope. The downlink beam returned from the retro-reflectors is ideally circularly polarized with the opposite handedness to the uplink beam. The QWP converts the downlink beam to linear polarization, rotated 90° with respect to the uplink beam. At the polarizing beam splitter, the beam is s-polarized, which results in the return beam being diverted to data collection and CCD detector channels.

2. Polarization effects of the OCTL optical system components

The mirrors in the OCTL system use two types of high-reflectance coatings. The mirrors on the laboratory table in the Coudé room use a reflection coating from Lambda Research, and the five 45° fold mirrors and the Cassegrain telescope mirrors use a Denton FSS99-500 protected silver coating. Denton provided JPL with a full set of calculated reflectance and phase data (P-S phase difference upon reflection) for the protected silver coating as a function of angle of incidence at both 532 nm and 1064 nm, while we were only able to receive corresponding data for P-S phase difference upon reflection for the Lambda Research coating at 1064 nm.

For our analysis, we substituted data for the Lambda Research reflective coatings with Denton coating data, since the Denton data showed a much larger variation in phase shift on reflection at 1064 nm versus angle of incidence than the Lambda Research coating and had lower reflectance at both 532 nm and 1064 nm. Thus, using Denton coating data for the mirrors on the laboratory table was likely to give worst-case performance and indicate whether these optics might contribute to polarization losses. The data for reflectance and P-S phase difference upon reflection are plotted in Figure 3.

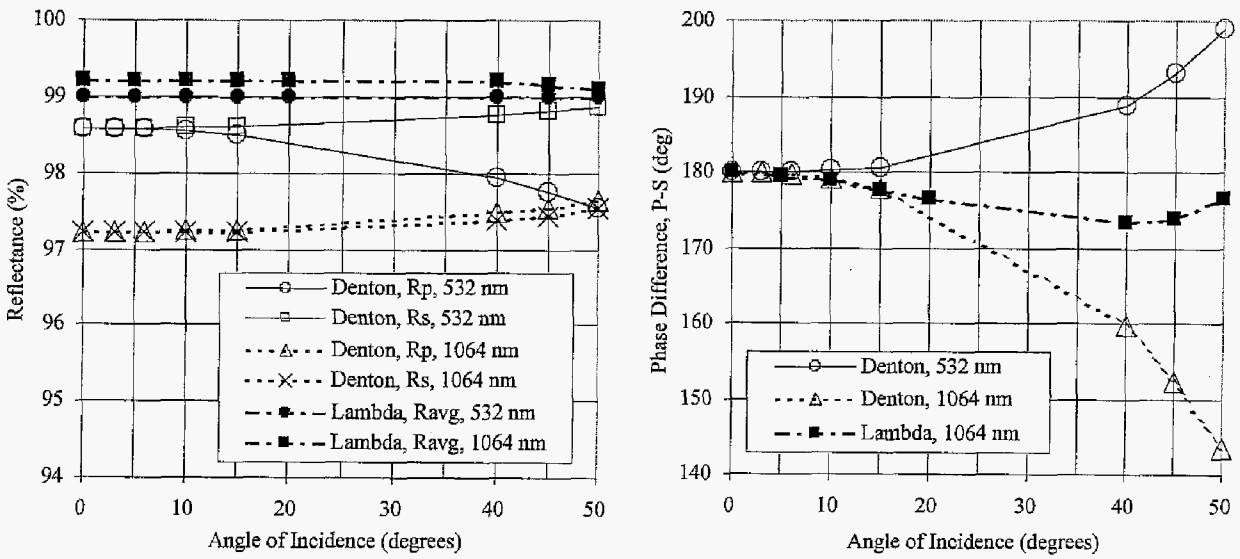

(a) (b)

Figure 3. Calculated values for (a) reflectance and (b) P-S phase difference upon reflection versus angle of incidence at wavelengths of 532 nm and 1064 nm for reflection coatings available from Lambda Research and Denton.

Figure 3(b) shows that both coatings provide a phase difference between p- and s-polarization states of approximately 180° near normal incidence (as desired). However, for mirrors used at 45°, the (P-S) phase difference varies significantly

from 180°, particularly for the Denton coating. Also, the sign of the phase difference changes if the source wavelength is changed from 532 nm to 1064 nm, indicating that the effects of the mirrors on the polarization state of the beam depend strongly on wavelength.

Thus, the largest polarization effects result from the 45° fold mirrors from M3 to M7. The Denton coating has phase differences of 180+13.0° at 532 nm and 180–27.6° at 1064 nm. The Lambda Research coatings have a phase difference of 180–6° at 1064 and higher average reflectance than the Denton coating (other data are not available). After five folds, the total maximum retardance produced by the Denton coatings is 65° at 532 nm and -138° at 1064 nm, corresponding to retardance values in units of the source wavelength of 0.18 waves and –0.38 waves, respectively.

Without compensation, these will significantly affect the polarization state, causing light to be lost upon return through the polarization beam splitter. As the mirrors are rotated as a function of telescope elevation and azimuth angles, it has the effect of a series of retarders rotated with respect to one another.

We analyzed polarization losses from the optics up to the telescope versus telescope tracking angle in double-pass. For this analysis, we modeled the retro-reflectors as a single ideal mirror following telescope in the uplink direction. Also, we did not include atmospheric effects or beam spreading after propagation. (The actual return beam may be spread out by hundreds of meters at the telescope.) Thus, the analysis approximates polarization losses due to the ground optics with a perfect retro-reflection. We have also analyzed the polarization effects of reflection from various types of retro-reflectors commonly used; however, those results are outside the scope of this discussion.

2.1 Polarization performance for all optical components excluding the 45° fold mirrors

Initially, we analyzed performance of the optical system from the laser to the telescope with the effects of the five 45° fold mirrors excluded. We found that the effects on the polarization of the beam from these components are very small. In the uplink direction, the beam is nominally circularly polarized following the quarter wave plate and before being reflected from Mirror M7.

If we define the polarization type, PTP, as the ratio of the intensity of the minor axis electric field component to the intensity of the major axis component for elliptically polarized light, then the polarization type may vary from zero for linearly polarized light to one for circularly polarized light. Prior to Mirror M7 in the uplink direction, we calculated values for PTP over the field and pupil of 0.9997 ± 0.0002 at 532 nm and 0.9993 ± 0.0004 at 1064 nm. Following the telescope, excluding the effects of Mirrors M3 to M7, we calculated values for PTP of 0.994 ± 0.005 at 532 nm and 0.975 ± 0.019 at 1064 nm. With a worst case PTP value of 0.956, the transmission loss following a QWP and analyzer is only 0.013%.

Thus, the variations in the polarization state produced by all the optical components other than Mirrors M3 to M7 are negligible. This is due to the fact that the light is linearly polarized at each of the mirrors on the laboratory table and either p- or s-polarized, so that the phase difference caused by the coatings does not significantly affect the polarization state. Also, the beam is close to normal incidence on the telescope mirrors, with a maximum angle of incidence of 8.5°, which gives a maximum P-S phase difference of only 0.36° (0.002 waves).

2.2 Polarization performance with the 45° fold mirrors

As we described above, the 45° mirrors together may produce as much as 0.18 waves of retardance at 532 nm and –0.38 waves of retardance at 1064 nm. Also, as the telescope tracks across the sky, the mirrors are rotated, which has a similar effect to a series of rotating retarders. As a result, we find that these mirrors contribute to significant polarization losses. As shown in Figure 2, four of the mirrors are rotated to change the telescope pointing direction. For elevation angle, M3 rotates relative to M7 and the M4 to M6 group. For azimuth angle, Mirrors M3 to M6 rotate as a group relative to the beam from Mirror M7.

In Figure 4, we plot the double-pass transmittance as a function of elevation and azimuth angles at wavelengths of 532 nm and 1064 nm for one of the four transmitted beams. The elevation angle may vary from 0° at the horizon to 90° at the zenith, and the azimuth angle may vary from 0° to 360°. As shown, the double pass transmittance varies significantly with pointing direction, and for a wavelength of 1064 nm, the transmittance can reach close to zero.

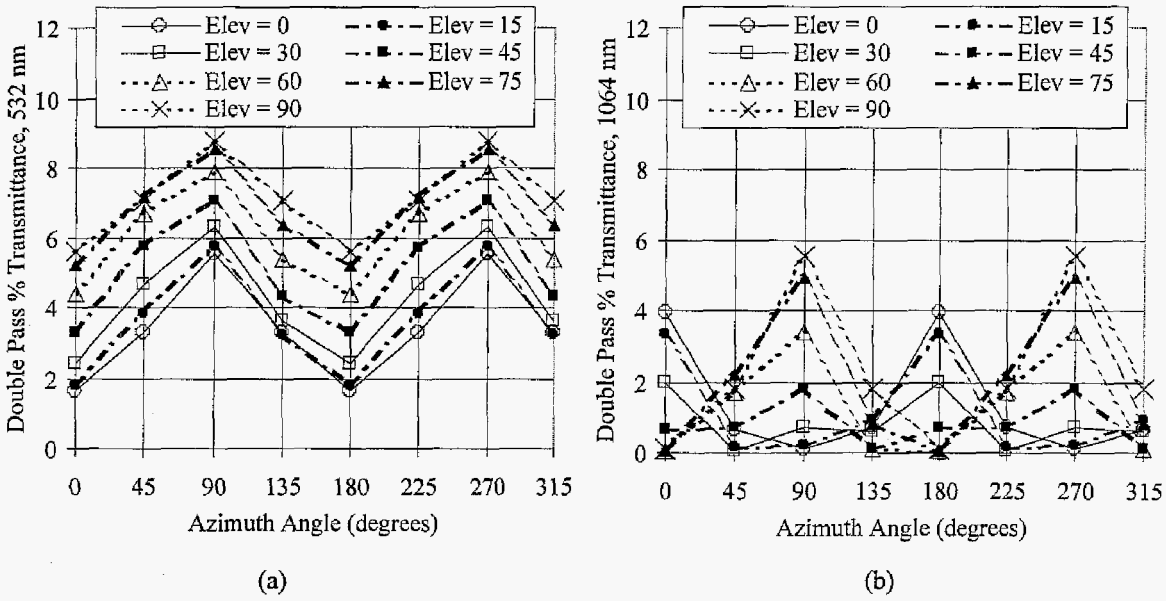

Figure 4, Double-pass transmittance for one of four transmitted beams in the OCTL optical system assuming a perfect retro-reflection at (a) $\lambda = 532$ nm and (b) $\lambda = 1064$ nm without polarization loss compensation.

3. Polarization loss compensation

As the mirrors are rotated as a function of telescope elevation and azimuth angles, they act as a series of linear retarders that are rotated with respect to one another. These retardance effects change the polarization state of the beam such that, when the beam is retro-reflected back through the optical system, some of the returning light will be lost at the polarization beam splitter that directs the return beam to the detector channels.

At $\lambda = 532$ nm, each mirror retards the s-polarization component relative to the p-polarization component, similar to a linear retarder with its slow axis along the tilt axis of rotation of the mirror. At $\lambda = 1064$ nm, the (P-S) phase difference is opposite in sign to the phase difference for $\lambda = 532$ nm, and the mirror behaves like a linear retarder with its fast axis along the tilt axis of rotation.

3.1 Custom wave plate compensation method

ORA initially proposed a straightforward method for compensating the retardance effects of the fold mirrors, in which a series of linear retarders would be used to provide an equal amount of retardance to the mirror or group of mirrors, but are aligned such that the retardance values cancel out.

In the OCTL system, there are five fold mirrors. Relative to the fast axis of the quarter wave plate between the Coudé room optics and the fold mirrors, Mirror M7 is fixed, Mirror M3 is rotated to provide elevation angle control, and the whole group of mirrors from M3 to M6 rotates for azimuth angle control.

We can compensate for the mirror retardance effects by using a set of three wave plates with custom retardance values. One of these custom wave plates is fixed to compensate for the retardance produced by Mirror M7, another custom wave plate rotates to compensate for Mirror M3 (which rotates as a function of elevation angle), and the third wave plate compensates for Mirrors M4 to M6 (which move with Mirror M3 as a group as a function of azimuth angle). A different set of wave plates is required at 532 nm and 1064 nm, since the retardance produced by the coatings varies with wavelength.

The M7 and elevation mirror (M3) compensators must compensate for retardance from a single mirror with a Denton coating, –0.03615 waves at 532 nm and 0.07670 waves at 1064 nm. Azimuth Angle is adjusted using a group of three mirrors, so the required retardance for the compensator for the azimuth mirror group is three times larger, –0.1085 waves at 532 nm and 0.2301 waves at 1064 nm. The order of the retarder compensators should be as shown in Figure 5, in

which the M7 compensator is adjacent to M7, the azimuth compensator is next to the M7 compensator on the laser side, and the elevation compensator is next to the azimuth compensator on the laser side. The angles of fast axes of the retarders are related to the elevation and azimuth angles as shown.

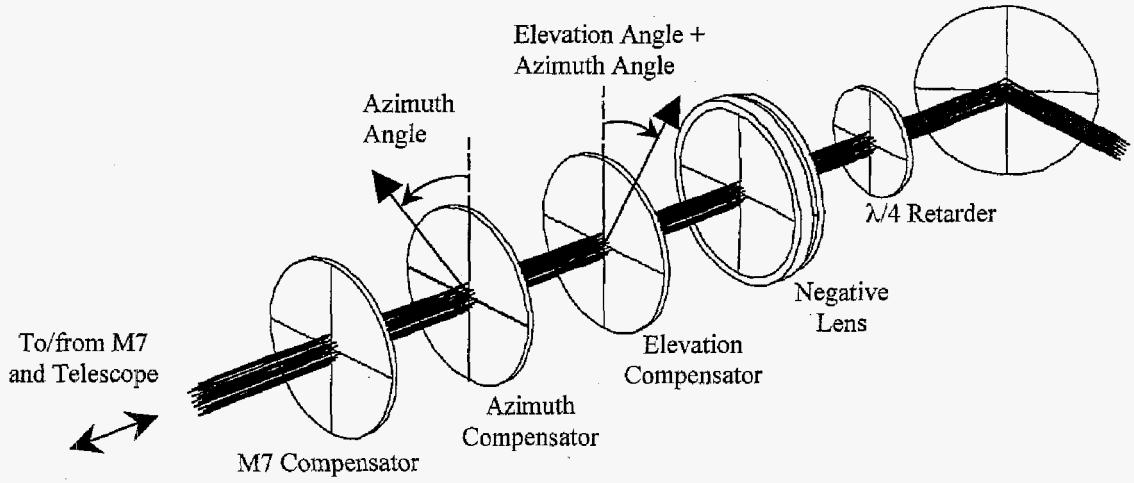

Figure 5. Arrangement of custom retarders for compensating the retardance effects of Mirrors M3 to M7.

Using CODE V[3] we analyzed the double-pass transmittance performance, averaged over the field of view and beam aperture, with coating prescriptions that model variations in reflectance and phase with angle of incidence to determine how effective the compensation is at the rotation values calculated using this method.

Figure 6 shows the double-pass transmittance of the OCTL system as a function of elevation and azimuth angles with compensation using the method shown in Figure 6 for one of the four transmitted beams. For the nominal system design (without the effects of tolerances), the retardance effects of the mirrors can be virtually eliminated; the calculated transmittance variation is less than ± 0.02% of the total double-pass transmittance at both source wavelengths. Thus, this approach is very effective for compensating the retardance effects of the mirrors.

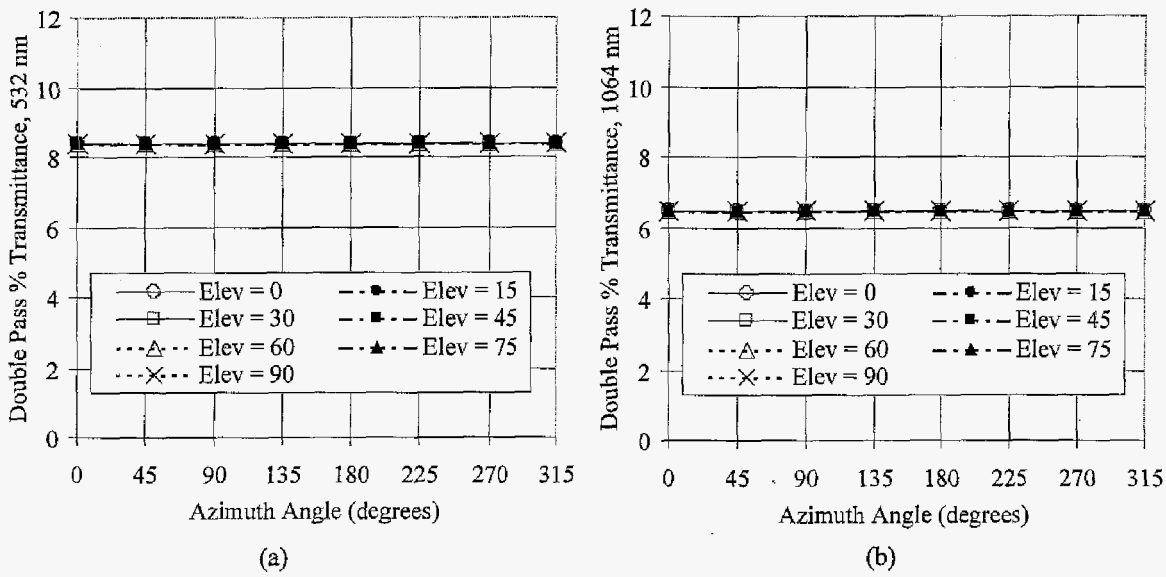

Figure 6. Double-pass transmittance for one of four transmitted beams in the OCTL optical system assuming a perfect retro-reflection at (a) $\lambda = 532$ nm and (b) $\lambda = 1064$ nm using the retardance compensation method described in Section 3.1.

However, this approach has some drawbacks. Each retarder must have a custom retardance value that is different for different source wavelengths. Also, the retardance values for wave plates that compensate the effects of a single mirror are small – only about $\lambda/28$ at $\lambda = 532$ nm or $\lambda/13$ at $\lambda = 1064$ nm. In practice, we found that it was difficult to locate a vendor that could produce the required retardance values with high accuracy at a reasonable cost. Also, there was a concern that the properties of the protected silver coated mirrors may differ from the values calculated based on the coating design. If the retardance values for the mirrors differed, there would be residual retardance errors that could not be compensated, resulting in variations in signal intensity as the telescope tracks across the sky. Because of these issues, we worked to implement a method that could use off-the-shelf components (typically with improved tolerances on retardance) and could accommodate unexpected errors in mirror coating retardance; this method is described in Section 3.2.

3.2 HWP/QWP retardance compensation method

To eliminate the drawbacks of the approach described in Section 3.1, JPL proposed a new method for retardance compensation. This method used a fixed quarter wave plate and two rotating quarter wave plates to cancel out the retardance effects of the 45° fold mirrors. In the uplink direction, the first, fixed QWP converts the linearly polarized input beam to circular. The second QWP is rotated to convert the circular polarization back to linear polarization, but rotated with respect to the linearly polarized input beam. Finally, a third QWP is rotated to convert the linearly polarized light following the second QWP to the desired elliptical state. This elliptical state is defined such that the retardance effects of the fold mirrors will convert the output beam to circular polarization.

ORA made a small modification to this approach to eliminate the fixed quarter wave. Instead, in the uplink direction, a half wave plate may be used to rotate the linearly polarized input beam to a desired rotation angle. Then, a QWP converts the linear polarization to the elliptical state required to compensate the retardance effects of the mirrors.

This method is similar to a general method that uses three wave plates in a QWP/HWP/QWP arrangement for converting any elliptically polarized input state to any elliptically polarized output state[1]. In the general method, the first QWP is needed to convert the input elliptical state to linear polarization, which is subsequently converted to the desired elliptical output state by the HWP/QWP pair. For the OCTL system, because the input beam is linearly polarized in the uplink direction, the first component of the QWP/HWP/QWP compensation method is not needed.

Therefore, our compensation method uses a HWP to rotate the linear input polarization and a QWP to produce the desired elliptical polarization such that the retardance effects of the mirrors will produce circular output polarization in the uplink direction. The rotations of both the HWP and QWP must be varied to compensate the effects of the mirrors. A schematic of the arrangement of compensating wave plates is given in Figure 7.

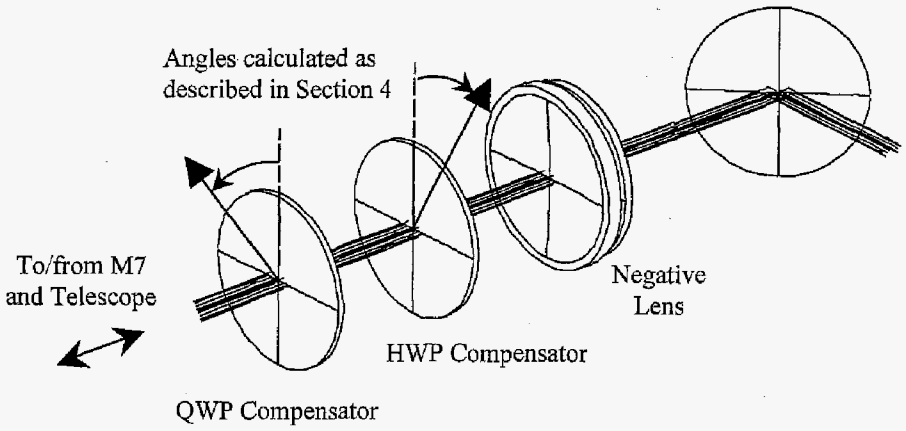

Figure 7. Half and quarter wave retarder arrangement for compensating the retardance effects of Mirrors M3 to M7.

The compensation method will also compensate the retardance effects of the mirrors in the return beam. The circularly polarized light, opposite in handedness, that returns through the system is converted to linear polarization by the compensating elements such that it is rotated 90° with respect to the linear input polarization in the uplink beam.

We modeled the use of this compensation method in CODE V and found that the double-pass transmittance varied by ± 0.04% of the total double pass transmittance at $\lambda = 532$ nm and ± 0.03% at $\lambda = 1064$ nm, and the plots showing double-pass transmittance versus elevation and azimuth angle are extremely similar to those shown in Figure 6. Thus, we have verified that this compensation method is effective over the full range of elevation and azimuth angles, and the transmittance variation for the nominal design is very small relative to JPL's goal (± 2.0% as-built transmittance variation).

In Section 4, we will describe an algorithm developed by ORA for calculating the required rotation angles for the HWP and QWP compensating elements as a function of telescope elevation and azimuth angles, as well as for wavelengths of $\lambda = 532$ nm and 1064 nm.

4.0 Wave plate compensator rotation angle calculations

In this section, we derive equations describing the required angular motions for the HWP and QWP compensating elements as a function of telescope azimuth and elevation angles and for wavelengths of $\lambda = 532$ nm and 1064 nm. As we will show, we were able to develop a relatively simple algorithm to directly solve for the rotation angles of the two wave plates. For our analysis, we used Mueller matrices and Stokes vectors to describe the polarization performance of the system. The analysis steps are as follows:

1. Start with the Stokes vector for the downlink beam, assuming it is circularly polarized (either left or right circular could be used; we selected left circularly polarized)
2. Calculate the Stokes vector after passing through each of the mirrors. Each mirror group is modeled using a Mueller matrix for a linear retarder, and rotation matrices are used to account for rotations of the elevation mirror and azimuth mirror group as a function of telescope pointing direction.
3. The downlink beam exiting from the group of mirrors will first pass through a quarter wave plate (QWP) to produce linear output polarization. Calculate the angle of the QWP to give linearly polarized output and the angle of the output polarization.
4. The linearly polarized beam from the QWP must pass through a HWP to rotate the polarization to be vertical (since the input beam is horizontally polarized in the uplink beam). The rotation angle of the HWP is calculated based on the angle of the output polarization from the QWP.

Step 1. Start with the Stokes vector for left circular input polarization, $\mathbf{S}_{input}$:

$$\mathbf{S}_{input} = \begin{bmatrix} 1 \\ 0 \\ 0 \\ -1 \end{bmatrix} \tag{1}$$

Step 2. Calculate the output polarization state following the group of mirrors:

Specify the matrices for the three mirror groups. The Mueller matrix for a general linear retarder with retardance, δ, is given by Eqn. 2:

$$\mathbf{M}_{retarder}(\delta) = \begin{bmatrix} 1 & 0 & 0 & 0 \\ 0 & 1 & 0 & 0 \\ 0 & 0 & \cos\delta & \sin\delta \\ 0 & 0 & -\sin\delta & \cos\delta \end{bmatrix} \tag{2}$$

Since the elevation and azimuth mirror groups rotate, we must apply rotation matrices to the general retarder Mueller matrix, where θ is the orientation of the fast axis:

$$\mathbf{M}_{retarder}(\delta, \theta) = \mathbf{R}(-\theta)\, \mathbf{M}_{retarder}(\delta)\, \mathbf{R}(\theta) \tag{3}$$

$$\mathbf{R}(\theta)=\begin{bmatrix}1 & 0 & 0 & 0\\ 0 & \cos(2\theta) & -\sin(2\theta) & 0\\ 0 & \sin(2\theta) & \cos(2\theta) & 0\\ 0 & 0 & 0 & 1\end{bmatrix} \tag{4}$$

Multiplying these matrices out, we get the following Mueller matrix for a linear retarder with fast axis rotation angle, θ, and retardance, δ:

$$\mathbf{M}_{\text{retarder}}(\delta,\theta)=\begin{bmatrix}1 & 0 & 0 & 0\\ 0 & \cos^2(2\theta)+\sin^2(2\theta)\cos\delta & \cos(2\theta)\sin(2\theta)(\cos\delta-1) & \sin(2\theta)\sin\delta\\ 0 & \cos(2\theta)\sin(2\theta)(\cos\delta-1) & \sin^2(2\theta)+\cos^2(2\theta)\cos\delta & \cos(2\theta)\sin\delta\\ 0 & -\sin(2\theta)\sin\delta & -\cos(2\theta)\sin\delta & \cos\delta\end{bmatrix} \tag{5}$$

The Stokes vector for the beam exiting the group of the mirrors for the return path is then given by Eqn. 6:

$$\mathbf{S}_{\text{mirror}} = \mathbf{M}(\delta_3,\theta_3)\,\mathbf{M}(\delta_2,\theta_2)\,\mathbf{M}(\delta_1,\theta_1)\,\mathbf{S}_{\text{input}} \tag{6}$$

Step 3. Calculate the rotation angle of the QWP to give linearly polarized output:

The Mueller matrix for a QWP at rotation θ is given by $\mathbf{M}_{\text{retarder}}(90°, \theta) = \mathbf{M}_{\text{QWP}}(\theta)$, as shown in Eqn. 7:

$$\mathbf{M}_{\text{QWP}}(\theta)=\begin{bmatrix}1 & 0 & 0 & 0\\ 0 & \cos^2(2\theta) & -\cos(2\theta)\sin(2\theta) & \sin(2\theta)\\ 0 & -\cos(2\theta)\sin(2\theta) & \sin^2(2\theta) & \cos(2\theta)\\ 0 & -\sin(2\theta) & -\cos(2\theta) & 0\end{bmatrix} \tag{7}$$

The output Stokes vector, S_{QWP} for the beam exiting the QWP is given by Eqns. 8 and 9:

$$\mathbf{S}_{\text{QWP}} = \mathbf{M}_{\text{QWP}}(\theta)\,\mathbf{S}_{\text{mirror}} \tag{8}$$

$$\begin{bmatrix}S_{0,\text{QWP}}\\ S_{1,\text{QWP}}\\ S_{2,\text{QWP}}\\ S_{3,\text{QWP}}\end{bmatrix}=\begin{bmatrix}1 & 0 & 0 & 0\\ 0 & \cos^2(2\theta) & -\cos(2\theta)\sin(2\theta) & \sin(2\theta)\\ 0 & -\cos(2\theta)\sin(2\theta) & \sin^2(2\theta) & \cos(2\theta)\\ 0 & -\sin(2\theta) & -\cos(2\theta) & 0\end{bmatrix}\begin{bmatrix}S_{0,\text{mirror}}\\ S_{1,\text{mirror}}\\ S_{2,\text{mirror}}\\ S_{3,\text{mirror}}\end{bmatrix} \tag{9}$$

For linear output polarization, the S_3 Stokes term (which defines the circularity of the polarization) must be equal to zero. Thus, we only need the equation for $S_{3,QWP}$ to determine the rotation angle for the QWP to give linear output polarization. The equation for $S_{3,QWP}$ is given in Eqn. 10.

$$S_{3,\text{QWP}} = -\sin(2\theta)\,S_{1,\text{mirror}} - \cos(2\theta)\,S_{2,\text{mirror}} = 0 \tag{10}$$

By setting this equation equal to zero, we can solve for the angle of the QWP fast axis, θ_{QWP}. The solution is given in Eqn. 11; the QWP angle is simply related to the inverse tangent of the ratio of the S_2 and S_1 Stokes vector terms following the group of mirrors. (Note that in programming this, the ATAN2 function should be used for $\tan^{-1}$ (y/x) to avoid divide-by-zero problems.)

$$\theta_{QWP} = -\frac{1}{2}\tan^{-1}\left(\frac{S_{2,mirror}}{S_{1,mirror}}\right) \tag{11}$$

This angle is input into Eqn. 9 to solve for the output Stokes vector, $\mathbf{S}_{QWP}$.

The rotation of the linear output polarization, θ_{linear}, from the QWP is then calculated using a similar equation given in Eqn. 12; this is the equation for the polarization azimuth angle (i.e., polarization orientation, POR, in CODE V) for a general Stokes vector, in which the angle is with respect to the Y-axis (in units of radians):

$$\theta_{\text{linear}} = \frac{\pi}{2} - \frac{1}{2}\tan^{-1}\left(\frac{S_{2,\text{QWP}}}{S_{1,\text{QWP}}}\right) \tag{12}$$

The beam then passes through the half wave plate (HWP), which rotates the linear polarization by twice the angle between the input polarization and the fast axis of the HWP. To produce vertical linear polarization, as desired in the OCTL system, we divide the polarization angle given by Eqn. 12 by two, as described by Eqn. 13 (in units of radians):

$$\theta_{\text{HWP}} = \frac{\pi}{4} - \frac{1}{4}\tan^{-1}\left(\frac{S_{2,\text{QWP}}}{S_{1,\text{QWP}}}\right) \tag{13}$$

To check these calculations, the full system matrix may be calculated, using Eqns. 14 and 15:

$$\mathbf{M}_{\text{total}} = \mathbf{M}_{\text{HWP}}(\theta_{\text{HWP}})\, \mathbf{M}_{\text{HWP}}(\theta_{\text{QWP}})\, \mathbf{M}(\delta_3, \theta_3)\, \mathbf{M}(\delta_2, \theta_2)\, \mathbf{M}(\delta_1, \theta_1) \tag{14}$$

For left circular input polarization, the result should be as given in Eqn. 15 (vertical linear output):

$$\begin{bmatrix} 1 \\ -1 \\ 0 \\ 0 \end{bmatrix} = \mathbf{M}_{\text{total}} \cdot \begin{bmatrix} 1 \\ 0 \\ 0 \\ -1 \end{bmatrix} \tag{15}$$

For this method, there are a few variations that may be useful. The quarter wave plate may be replaced by a three-quarter wave plate. For calculating the rotation angles, a retardance of 270° would be used rather than 90°. Also, note that it is allowable to add multiples of ± 180° to the calculated QWP rotation angle or ± 45° to the calculated HWP rotation angle. If the parts can be rotated continuously in the same direction, this may be used to maintain a constant rotation direction.

We provide plots of the HWP and QWP rotation angles as a function of telescope elevation and azimuth angles in Figures 8 and 9 (based on the particular coordinate system definitions that we used for the CODE V optical system model). In Figures 8 (a) and (b), the HWP and QWP rotation angles, respectively, are plotted at $\lambda = 532$ nm, and similar plots are given for the HWP and QWP rotation angles for $\lambda = 1064$ nm in Figures 9 (a) and (b). The HWP rotation angles vary between -90° and 0°, and the QWP rotation angles vary between -90° and 90°. As mentioned earlier, it is allowable to add multiples of ± 180° to the calculated QWP rotation angle or ± 45° to the calculated HWP rotation angle.

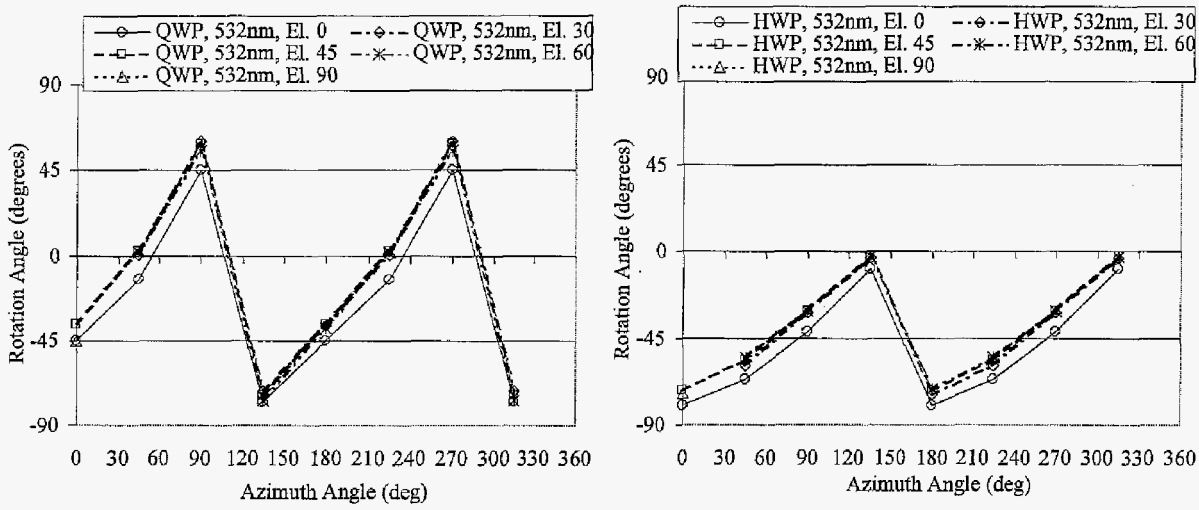

Figure 8. Rotation angle for the fast axis of the (a) HWP and (b) QWP compensating elements relative to 0° along the vertical system Y-axis versus telescope elevation and azimuth angles at $\lambda = 532$ nm. Multiples of ± 45° may be added to the HWP rotation angles, and multiples of ± 180° may be added to these QWP rotation angles.

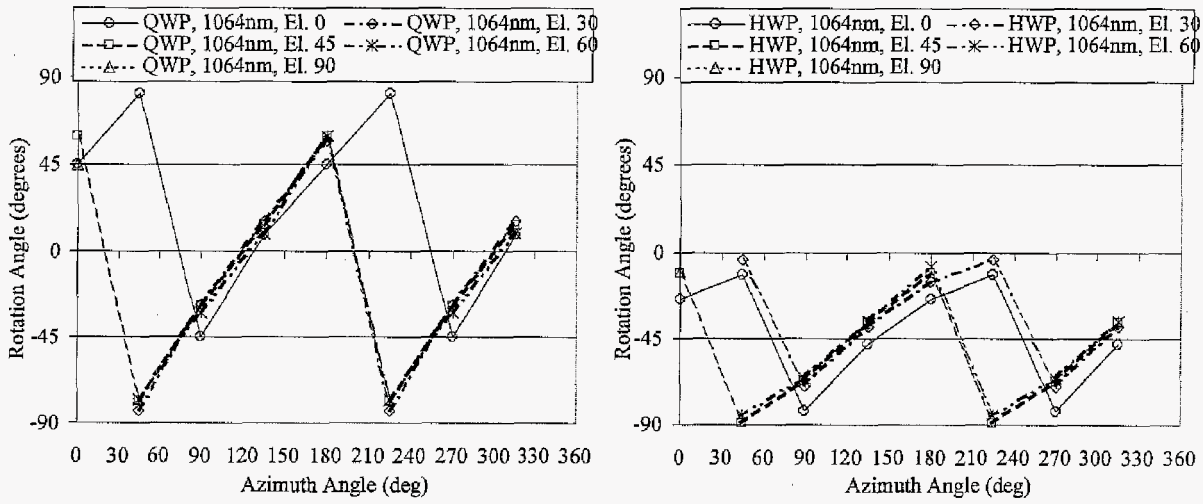

Figure 9. Rotation angle for the fast axis of the (a) HWP and (b) QWP compensating elements relative to 0° along the vertical system Y-axis versus telescope elevation and azimuth angles at $\lambda = 1064$ nm. Multiples of ± 45° may be added to the HWP rotation angles, and multiples of ± 180° may be added to these QWP rotation angles.

5. Conclusions

We have analyzed polarization performance of a sky-tracking laser transceiver system being developed by the Jet Propulsion Laboratory and found that a group of five 45° fold mirrors with protected silver coatings used in the elevation/azimuth telescope mount produce significant amounts of polarization retardance. These retardance values lead to polarization losses as the telescope tracks across the sky, as well as with source wavelength, and can result in nearly a total loss of the return signal retro-reflected from a cube-corner equipped Earth-orbiting satellite at some tracking angles.

We described two approaches for compensating these retardance effects. The most direct approach is to use a series of three linear retarders to cancel out the retardance effects of the mirrors, including one fixed retarder to compensate for

a fixed mirror and two rotating retarders to cancel out the retardance effects of the mirrors that are rotated as the telescope pointing direction is changed. This approach requires custom retardance values that are difficult to acquire with tight retardance error tolerances, and there is no means to account for errors in the estimated retardance values produced by the mirrors.

We described a second, improved compensation approach that uses only two retarders, a quarter wave plate and a half wave plate (two fewer wave plates than the custom wave plate approach, since the original QWP can be eliminated). These retarders are mounted in rotation stages and are rotated to provide the necessary retardance correction. We have provided an algorithm for analytically calculating the required retarder rotation angles to use as the telescope tracks across the sky.

This method allows the use of off-the-shelf components. Furthermore, during alignment of the system, the angles of the retarders can be adjusted to maximize a return signal to determine the actual retardance values of the protected silver coated mirrors, and the algorithm for rotating the wave plates can be adjusted to maximize transmittance and minimize variation with telescope tracking angle. This also provides the ability to adjust the polarization correction system to correct for any future changes in the polarization characteristics of the OCTL telescope optical train such as coating deterioration, a coating being replaced with a new one, or changes in optical alignment.

6. Acknowledgments

The work described in this paper was performed by the Jet Propulsion Laboratory, California Institute of Technology, and Optical Research Associates under contract with the National Aeronautics and Space Administration. The authors would like to acknowledge the contributions of Dr. Keith E. Wilson for his support of this work.

7. References

1. S. Yao, "Polarization in Fiber Systems: Squeezing Out More Bandwidth," *The Photonics Handbook 2005, Book 3*, (Laurin Publishing, Pittsfield, Mass., 2005)
2. K. E. Wilson, Planned Operations for the JPL Optical Communications Telescope Laboratory (OCTL), http://lasers.jpl.nasa.gov/PAPERS/OCTL/crl02.pdf, January, 2003.
3. CODE V® is a registered trademark of Optical Research Associates, Pasadena, California
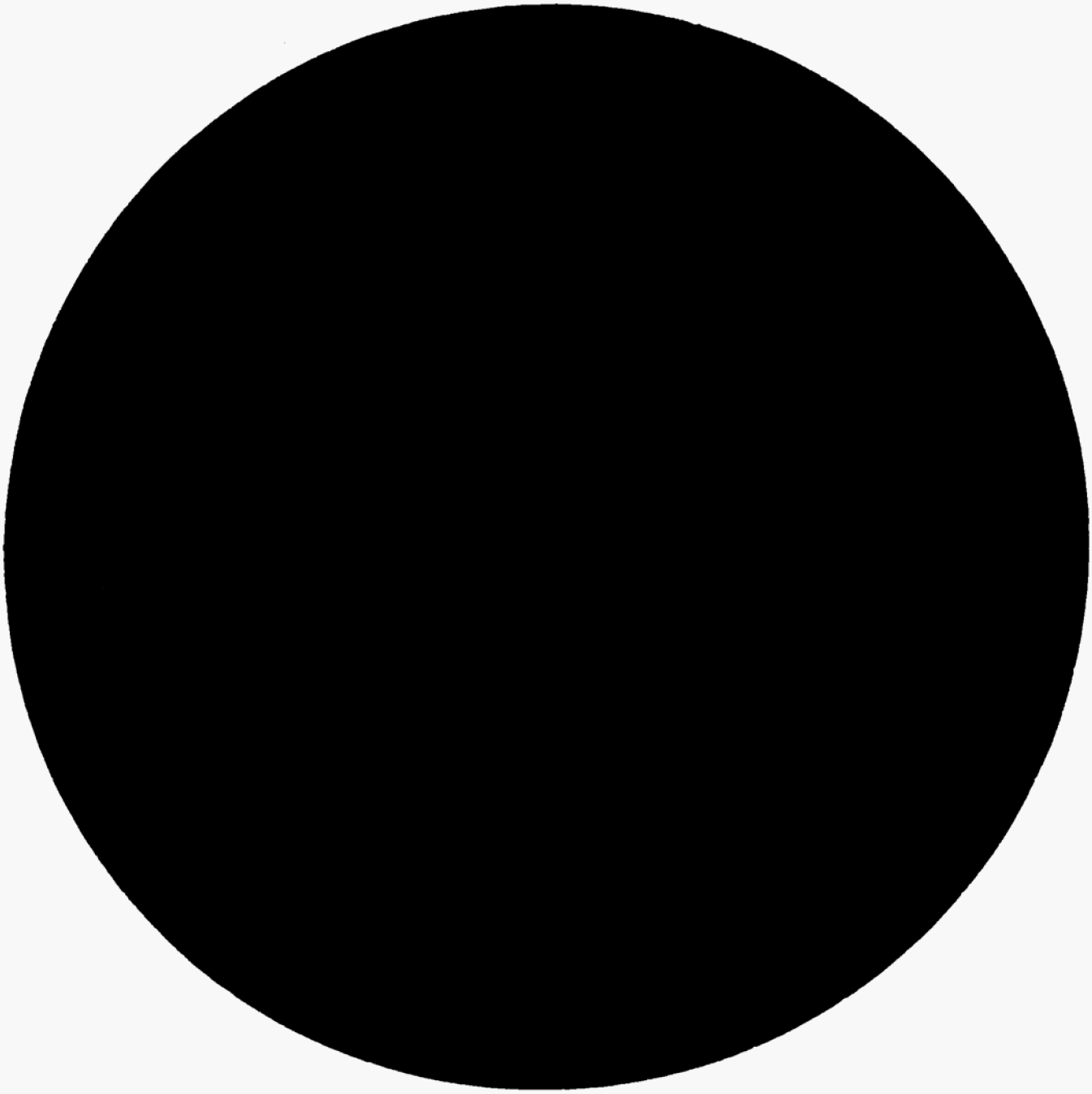
End of File